International Journal of Mechanical, Industrial and Aerospace Sciences
ISSN: 2517-9950
Vol:9, No:1, 2015

Investigations on the Influence of Optimized Charge Air Cooling for a Diesel Passenger Car

Christian Doppler, Gernot Hirschl, Gerhard Zsiga

***Abstract*—**Starting in 2020, an EU-wide CO_2-limitation of 95 g/km is scheduled for the average of an OEMs passenger car fleet. Taking that into consideration additional improvement measures of the Diesel cycle are necessary in order to reduce fuel consumption and emissions while boosting, or at the least, keeping performance values at the same time.

The present article deals with the possibilities of an optimized air/water charge air cooler, also called iCAC (indirect Charge Air Cooler) for a Diesel passenger car amongst extreme-boundary conditions. In this context, the precise objective was to show the impact of improved intercooling with reference to the engine working process (fuel consumption and NO_x-emissions). Several extreme-boundaries - e.g. varying ambient temperatures or mountainous routes - that will become very important in the near future regarding RDE (Real Driving emissions) were subject of the investigation. With the introduction of RDE in 2017 (EU6c measure), the controversial NEDC (New European Driving Cycle) will belong to the past and the OEMs will have to avoid harmful emissions in any conceivable real life situation.

This is certainly going to lead to optimization-measurements at the powertrain, which again is going to make the implementation of iCACs, presently solely used for the premium class, more and more attractive for compact class cars. The investigations showed a benefit in FC between 1 and 3% for the iCAC in real world conditions.

***Keywords*—**Air/Water-Charge Air Cooler, Co-Simulation, Diesel Working Process, EURO VI Fuel Consumption.

I. Turbocharging & Charge Air Cooling from the Thermodynamic Point of View

NOWADAYS the majority of passenger cars and commercial vehicles is equipped with intake air charging systems in order to raise efficiency and power output. Via the compression of air in the charging system an increase of the working fluid's pressure and temperature level is taking place. Thereby a rise of enthalpy occurs as illustrated in the δH/δs-diagram in Fig. 1.

For an ideal compressor, this is called isentropic compression, which means that there is no heat exchange to the surroundings (adiabatic process) as it is described by the black vertical line in the diagram parallel to the y-axis. Due to its irreversible process property which implicates a raise in fluid's temperature, a real compressor needs to deliver an extended amount of power to compensate losses. This effect can be characterized with the increase of entropy which is seen as a thermodynamic loss, illustrated with state b* in the diagram. It can be noticed that b and b* have the same level of pressure which consequently illustrates that it is highly favorable to reach state b.

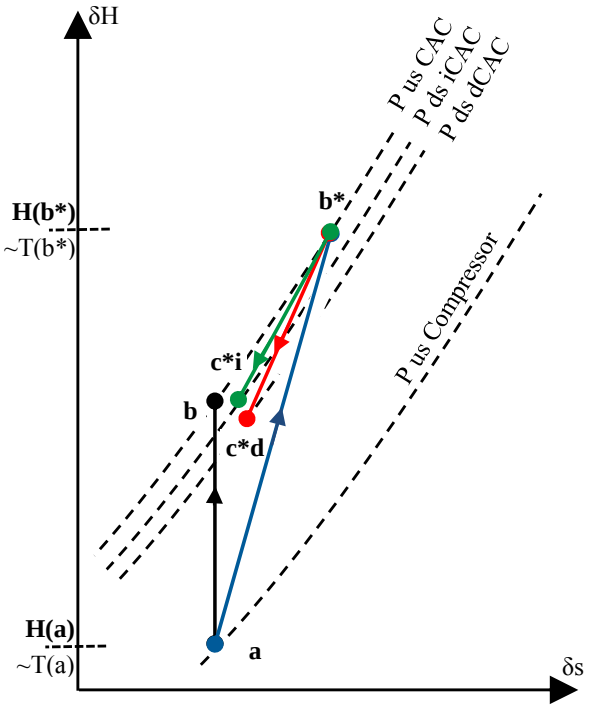

Fig. 1 δH/δs Diagram for Turbocharging and Intercooling

An intercooling system can partly compensate losses and leads to an increase of the isentropic total efficiency of the turbocharging system by a reduction of the enthalpy-difference in comparison to state b*.

The state change to c*d (intercooling via direct CAC) describes a higher loss in pressure, as this occurs with an indirect CAC (due to a more compact heat exchanger architecture), which can be seen at c*i.

However, it must be mentioned that this is just a schematic diagram to describe the principles; especially the curves *P ds dCAC* and *P ds iCAC* are situated much closer in reality.

Since the intercooling is responsible for an outlet temperature similar to the inlet temperature at the intake system (turbocharger/CAC) - this enables a rather isothermal

Christian Doppler is with the Virtual Vehicle Research Center, Inffeldgasse 21A, 8010 Graz, Austria (phone: +43(0)316/873 9803; e-mail: christian.doppler@v2c2.at).

Gernot Hirschl is with the AVL List GmbH, Hans-List-Platz 1, 8020 Graz, Austria (phone: +43(0)316/7870, e-mail: gernot.hirschl@avl.com).

Gerhard Zsiga is with the MAHLE Behr GmbH & Co. KG, Mauserstr. 3, 70469 Stuttgart, Germany (phone: +49(0)711/501 47686 e-mail: gerhard.zsiga@mahle.com).

compression which results in the well-known benefits of higher volumetric efficiency in the combustion process.

By the implementation of a low temperature water circuit, the distinctly higher ability of water for rejecting heat in comparison to air is used. While at standard conditions air solely has a c_p-value of 1.005 kJ/kgK, the value for water is 4.182 kJ/kgK. This difference becomes remarkable, especially when comparing the conductive cooling power of an air cooling system with a water cooling system.

Therefore, Table I gives an overview of different cooling approaches and their proper HTCs (Heat Transfer Coefficients) [1]:

TABLE I
HTC FOR DIFFERENT COOLING SYSTEMS

Technology	HTC [W/m^{2}K]
Free convection of air	5-30
Free + forced convection of air	20-400
Forced convection water	100-1600
Immersion chilling	800-10000

In [1] an example for convection-cooling is performed with cooling a 100cm^2 plate with a δT of 30K, illustrated with Newton's law of cooling in (1).

$$\delta Q = \alpha * A * (T2 - T1) \quad (1)$$

δQ: heat flow from plate to cooling medium in W; α: heat transfer coefficient in W/m^{2}K; A: surface area in cm^2; T2: temperature of plate in K; T1: temperature of fluid in K.

While forced air cooling with a maximum HTC of 400 leads to 120W of heat loss, the rate of heat loss may ascend up to 3000W via water immersion chilling.

Summing up, it can be said that water cooling is a potential enabler for the improvement of cooling efforts.

Several studies conducted in the past demonstrated the potentials and challenges regarding charge air cooling by the aid of low temperature water circuits [3], [4]. The major benefits that appeared in those studies are undeniably a better transient performance as well as a higher volumetric efficiency.

As this leads to a high potential for power enhancement, different passenger vehicles (firstly gasoline engines) in the premium/high-end class have been equipped with water/air CAC systems since 2007 [3]. Examples for a successful realization are the Mercedes M 278 engine, installed in the S- and CL-class or the BMW N63, driving the 5 series and the X5. Both variants are built in the v-form with biturbo charging that strongly offers the space saving integration of the water/air CAC within the V-housing.

Latest research results even show potential for single stage turbocharged Diesel engines on heavy duty trucks with a significant reduction of fuel consumption in the NEDC [5].

II. Background to the Used Approach of Engine Modelling

The basis for the investigations was the preparation and simulation with an appropriate engine model. Therefore, the combustion engine process can be modelled with different simulation approaches which are distinguished mainly by the spatial discretization, which again influences the simulation time:

A. 3D/Multi-Dimensional Method

Calculation of detailed flow processes by means of continuity equation as well as Navier-Stokes equations [2]

B. 1D/Phenomenological Method

Multi-zone calculation, each zone representing physical and chemical phenomena's

C. 0D/Quasi-Dimensional Method

Thermodynamic calculation with respect to conservation of mass & energy, without flow-field modelling

D. Non-dimensional Method

Neuronal, polynomial & mean value models which are without physical background information

Whereas the detailed granularity for a 3D CFD calculation leads to a RTF (real time factor) of 10000+, on the other hand a non-dimensional calculation gains RTFs precisely below 1.

In this work, the combination of a 0D/1D simulation environment was chosen as basis for the investigations (RTF 50-1000).

The calculations in this method are commonly performed with crank-angle-resolved time steps which allow the analysis of a reciprocating engine very into detail. In terms of the Diesel engine, this level permits the illustration of the gas exchange (influx, exhaust & leakage), the mixture preparation, the combustion as well as the heat losses.

Investigations were performed on a Diesel engine of the 40 kW/l class with low pressure EGR (Exhaust Gas Recirculation) and a *variable-geometry* turbocharger.

As simulation tool AVL BOOST® was used. According to that method, the gas exchange outside of the cylinder is calculated one-dimensionally with the implementation of continuity-, momentum- and energy-equations. This enables a detailed consideration of changes in the intake air system caused by different charge air cooling concepts. On the other side, a *single-* or *multi-zone* 0D method describes the combustion process itself with the aid of physical and empirical approaches.

Due to the fact that the formation of NO_x has an exponential dependence on the burning zone temperature, a multi zone combustion approach was used in order to analyze zones of different temperatures and mixture. The quasi-dimensional calculation does not only support the determination of a single-zone 0D approach but also a determination of user-defined zones to distinguish between burned and unburned area.

By utilizing the 2-Zone combustion model, the calculation of proper temperatures for both zones was enabled [6]. As basis, tables with the load-point-specific ROHR (Rate of Heat Release) [1/deg] are allocated by test bed measurement.

Considering e.g. an engine rotational speed of 2000 rpm, this results in 12000 single degrees (=calculation steps) per

second. This detailed granularity highly complicates a simulation that also takes into account superior elements like the whole powertrain or the environment. With an optimistic RTF of 30, solely one parametric study for a 1200 s lasting NEDC (New European Driving Cycle) leads to a simulation time of 10 hours.

In order to enable arguable investigations, a simplification of the modelling depth was inevitable.

This was achieved by assuming that any thermodynamic change is taking place during one working process. That course of action permits the significant simplification to calculate with averaged values along one working cycle. By means of this method, it was supposed that the input conditions do not change drastically during one single working cycle. Accordingly, in comparison to the thermodynamic cycle calculation, the computing time can be decreased drastically.

III. Engine Model Simplification

As the object of studies was to take investigations on different CAC-variants, the engine unity was split up into EP1 (Engine Part I) and EP2 (Engine Part 2) in order to implement the CAC into the engine. This properly developed approach enables the possibility to benchmark different cooling variants in a very fast way via flexible integration into the engine on the basis of a co-simulation.

Firstly, EP1 delivers the necessary intake air conditions downstream of the turbocharger and upstream of the CAC as seen in (2).

$$AIR, P\_21, T\_21 = f\,(N, Ped) \tag{2}$$

$\dot{m}_{AIR}$: Mass Flow Intake Air in kg/s; P_21: Pressure upstream of CAC in Pa; T_21: Temperature upstream of CAC in K; N: Engine Speed in 1/min; Ped: Pedal Position.

It must be mentioned that any bidirectional interactions between EP1 and CAC (like different pressure gradients or changing temperature profiles dating back from the CAC) were modelled. As in a first study the effort for additional modelling of such a side effect via a mean value model was regarded as inappropriate, it has been neglected out of necessity. Anyway, it is assumed that the influence is of minor weight and that it will not contribute to the relative simulation results consequently.

After the compressed fluid leaves EP1, a heat exchange is taking place within the CAC-model (explained later in detail) resulting in the essential state of compressed and cooled air which is streaming into the combustion engine modeled via EP2.

Thus, EP2 takes into account varying parameters in the intake plenum with the influences on the engine process. The effects of different CAC variants can be described by proper pressure losses along the CAC ($1\ldots5*10^3$ Pa) and temperature profiles (292.15…369.15K) in the intake manifold.

The number of sampling points was chosen high enough to illustrate the partly nonlinear effects of variations. Between the sampling points a linear integration leads to insignificant errors which do not affect simulative results. In conclusion, the mean value engine model EP2 can be described for different engine speeds and loads with (3).

$$FUEL, NOx, PWR, MD = f\,(N, Ped, \Delta pCAC, T\_2\_1) \tag{3}$$

$\dot{m}_{FUEL}$: Mass Flow Fuel in kg/s; $\dot{m}_{NOx}$: Mass Flow Nitrogen Oxide in kg/s; PWR: Engine Power in kW; MD: Torque in Nm; ΔpCAC: Pressure Prop along the CAC in Pa; T_2_1: Outlet Temperature CAC in K.

At part load, the simulations include a control in order to maintain the same power output with different ΔpCAC and T_2_1 levels. This was achieved via the use of the *BMEP Control Function* in *AVL BOOST*® which means that the injected fuel is varied with a PI control. Thus, it can be noticed that the AFR (air/fuel ratio) is changing constantly at part load with different boundary conditions on the basis of this control.

In addition, a control of the EGR was implemented (with the *low-pressure EGR flap*) to keep the NO_x emissions always on a constant level at different intake conditions.

At full load, an AFR-control was established. By keeping the AFR at a well-defined level, the compliance with soot emissions as well as highest efficiencies was realized.

IV. Powertrain Model

The overall powertrain and the environment were designed on the basis of *AVL CRUISE*®. The ability of modelling the longitudinal dynamics of the powertrain and the ambient conditions enables different use case studies. Further parts of the model are wheels, gearbox, gearbox-control, driver, clutch, differential and a torque flange for the input torque of the engine model.

The driving routes of the simulated cycles were also defined in *AVL CRUISE*® via a desired velocity profile which can be aligned either on a time or on a distance basis. For the parameterization of the real driving cycles, it turned out that the use of a distance profile is advantageous as this allows the reduction of driving velocity with respect to curvatures inter alia.

AVL CRUISE® has a driver element that conducts the vehicle speed control in order to correlate the actual velocity with the desired velocity. The tuning of this element in connection with the whole co-simulation environment was executed with a PI-control on the basis of a NEDC.

V. CAC Model

The quasi-stationary HX (heat exchanger) models are built in MAHLE's In-House Tool *BISS* (Behr Integrated System Simulation). This 1D-simulation-tool allows the calculation of the entire fluid system in a vehicle. In the present investigation, different HX from this library were implemented into the simulation environment. Herewith, the cores, as well as the manifolds of the HX are modelled with several zones on a 1D-basis. From the thermodynamic point of view, each of those zones is calculated separately. Ultimately,

the heat exchange is modeled via conduction. Therefore a HTC calculation is conducted on the basis of similitude variables. More information about *BISS* can be found in [7].

Two different variants of a dCAC as well as two iCAC-varieties have been examined closely. Table II gives a short overview of the HX-mesh and the circuity. While the dCAC is naturally built in cross flow form, the iCAC was realized in counter flow arrangement as this form supposes a higher efficiency in general. The installation height of an iCAC is solely about 15 % in comparison to a dCAC - as seen in the schematic illustrations in Fig. 2.

TABLE II
TECHNICAL DETAILS OF CAC-VARIANTS

Type	*Direct CAC (dCAC)*	*Indirect CAC (iCAC)*
Pipes	10	14
Geometries of Mesh W x H x D	157.4x660x64 mm	144.3x97x64 mm
Circuity	cross flow	counter flow
Pipe Frequency Outside	59/dm	33/dm
Pipe Frequency Inside	47/dm	110/dm

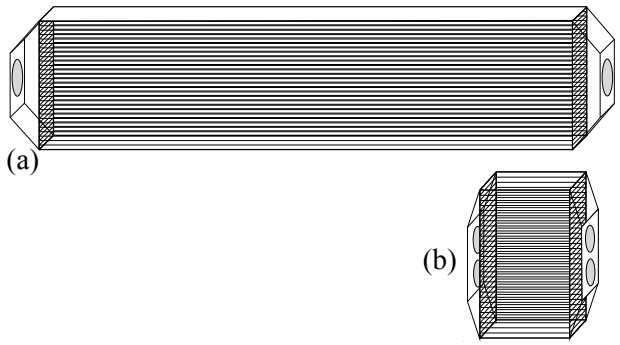

Fig. 2 HX-Size For dCAC (a) and iCAC (b)

VI. EXTENDED ICAC MODEL

Since the available iCAC model consists solely of a single HX, a further model was constructed, which represents the whole low temperature cooling circuit. The modelling took place on the basis of a validated thermodynamic library in *Matlab/Simulink*®, which is described in detail in [8]. Here, the dimensioning of the pipes and front HX was executed on the basis of utilizing MAHLEs experience.

Subsequent, the parameterization of the heat conduction for the *fin-tube HX* at the car's front end was performed. For this reason, the HTC for the air side is calculated on the basis of a nusselt correlation according to *Chang-Wang*, while the coolant heat transfer model is based on a Nusselt correlation from *Gnielinski* [8]. Further, a lumped mass was integrated into the car's environment in order to roughly map the thermal inertness of the surrounding engine compartment.

VII. CO-SIMULATION

For the overall simulation, an independent co-simulation platform (*ICOS*®) - developed at the Virtual Vehicle - was utilized. This tool enables a very quick and easy coupling of different simulation instruments. It is of great advantage that every tool operates with its proper simulation step size, while an appropriate information exchange between different models is executed.

ICOS® has a BCS (Boundary Condition Server) that allows the setting of time traces and constants as external values which are accessing the particular models. By doing so it is easy to tune controllers like the P- and I-values of the driver for optimal ride characteristics - always in the context of the re-influences of the whole co-simulation. Fig. 3 shows the model landscape for the final simulation environment, containing the models as well as the exchanged channels. On the left side of the diagram you can see the co-simulation environment which acts as exchange platform between the models on the right side. The interchanged channels are illustrated with the particular bolts. The following diagram shows the base principle of this interchange (without detailed information about the interchanged information).

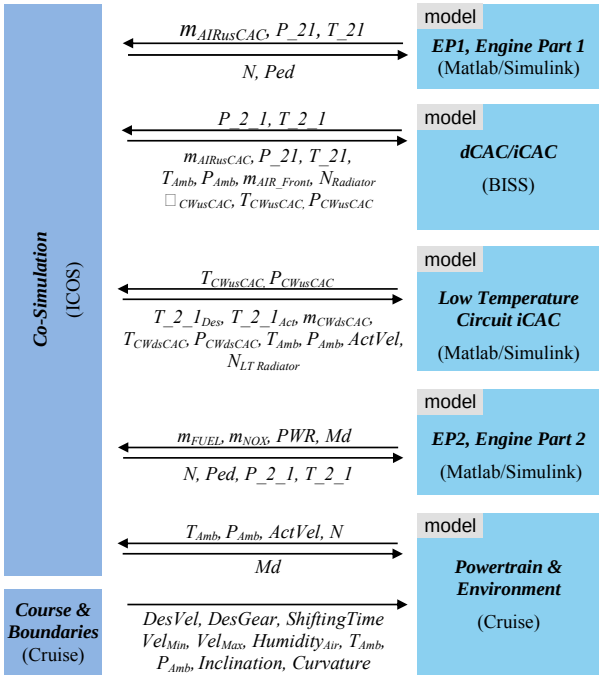

Fig. 3 Entire Environment of Co-Simulation

VIII. BASIC INVESTIGATIONS FOR TIPIN-TIPOUT

A basic investigation took place in a *TipIn-TipOut* cycle which should reveal information about the model quality as well as about the influences of the different HXs on the engine.

In a first step, the cooling water flow of the LT-Cycle (iCAC) was controlled in order to gain exactly the same temperature as with the dCAC – this procedure can be seen in

Fig. 4. Solely on the basis of a different pressure drop but without a better cooling performance, the fuel consumption of the system with an iCAC cropped up by 0.33 %.

The same test for the iCAC was done with a nominal temperature downstream the CAC of 25°C which enabled a more significant fuel benefit by 3.52%.

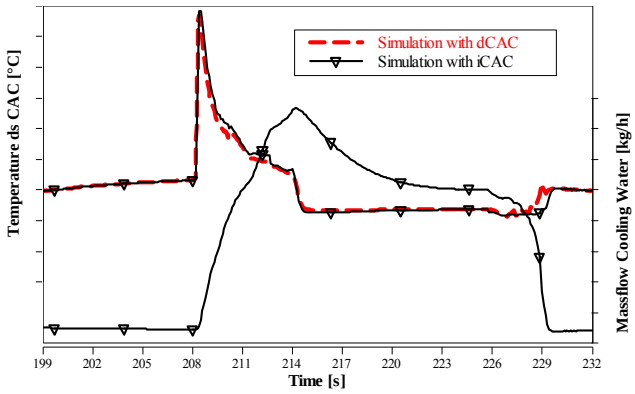

Fig. 4 Control of Temperature ds CAC via Mass Flow

IX. Comparison of Pressure Drop at Simulation with Testbed Results

To validate the CAC variants, measurements on the engine testbed have been conducted. The tests for the iCAC were performed on a 60 kW/l engine with an indirect CAC from MAHLE that was integrated into the intake plenum (integrated indirect CAC = i²CAC). The tests with the dCAC-variant were performed with an air/water HX that has the same pressure drop properties as a conventional air/air CAC.

Fig. 5 shows the pressure drops for every engine speed at full load. It can be seen an increase towards higher speeds and partly a relative good conformity of simulation with experimental data. The differences occur because the compared engines and coolers are slightly differing. But it can be remarked, that pressure loss characteristics for an iCAC respectively a dCAC are not significantly changing between different up-to-date engines and cooler variations.

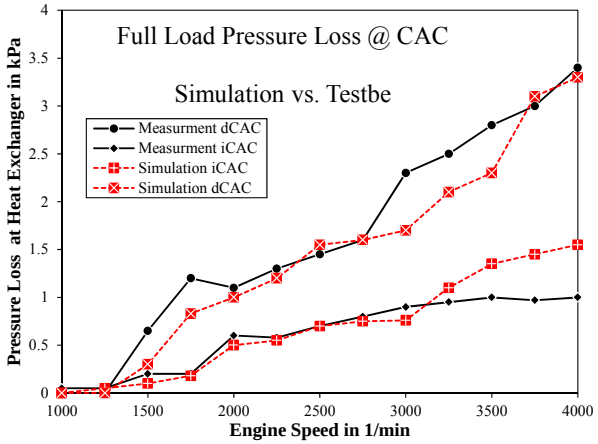

Fig. 5 Pressure Loss for Experimental & Simulative Results

X. Simulation of the NEDC

The actual European homologation cycle NEDC was performed with the simulation models amongst standard ambient conditions. Fig. 6 shows the dissipated quantity of heat for the simulations. For the iCAC-variant, the dissipation of heat is by 11% higher compared to the dCAC-variant. This leads to lower temperatures downstream the iCAC with 23.8°C in the middle, while the mean temperature downstream the dCAC is 29.8°C. In the simulations with the dCAC it could have been seen very high temperatures downstream the CAC during acceleration, those who led to the heat quantity gap, compared to the iCAC, as seen in Fig. 6. On the other hand, the iCAC enables a very flatten temperature profile for the intake air of the engine which results in more dissipated heat quantity.

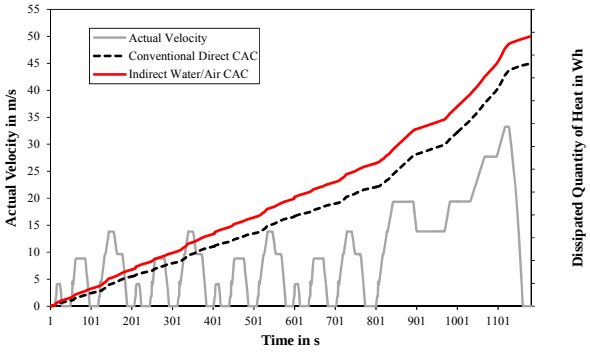

Fig. 6 Dissipated Quantity of Heat at the CAC for the NEDC

It must be mentioned that the very low temperatures at the intake air plenum might lead to condensation of the augmented proportion of water due to low pressure EGR (Exhaust Gas Recirculation). On the test bed, the same engine as in the simulations was operated for several hundred hours with the same outlet temperatures and it was not seen any damage to it. Anyway, it must be beard in mind that the water within the pipes will have led to corrosion. This problematic can be solved with appropriate water-separation devices in the HX (e.g. discharge outlet).

Equation (4) shows the formula for the ADR (*air density recovery*, which illustrates the total efficiency of a CAC with respect to the temperature drop (cooling power) as well as to the pressure drop. In the NEDC, the iCAC has an ADR value of 0.97 which is a particularly good performance, while the dCAC remains at 0.88.

$$ADR = \eta_\rho = \frac{\Delta\rho Air}{\Delta\rho Air, max} = \frac{\frac{TAir,In}{TAir,Out} * \left(1 - \frac{\Delta pAir}{pAir,In}\right) - 1}{\frac{TAir,In}{TCool,In} - 1} \quad (4)$$

In Table III an overview of the fuel consumption and the NO_x emissions is illustrated. Because the NEDC does not have any high-transient parts, the FC benefit for an iCAC is low with 0.8 %.

TABLE III
NEDC CYCLE RESULTS

		Direct CAC	Indirect CAC
∑ Fuel Consumption	g	653.28	647.90
∑ NO_x Emissions	mg	1078.71	1042.23
FC	g/km	59.69	59.20
NO_x	mg/km	98.57	95.22
FC	l/100km	7.19	7.13
CO_2	g/km	189.87	188.29
FC Benefit for iCAC	%		-0.83
NO_x Benefit for iCAC	%		-3.50

XI. Simulation of a Road with 30° Inclination and the Großglockner Parameter Studies

It is supposed, that the greatest advantage for a high performance charge air cooling is to be seen in a mountainous track with high torque demands and low air streams at the front end of the car.

In a first step, a steady state operation point with 30 % of inclination was chosen as this can be seen in Fig. 7. For comparison, the steepest road in the world can be found in New Zealand and has an inclination of 35 % (19.3°) – grey line in Fig. 7.

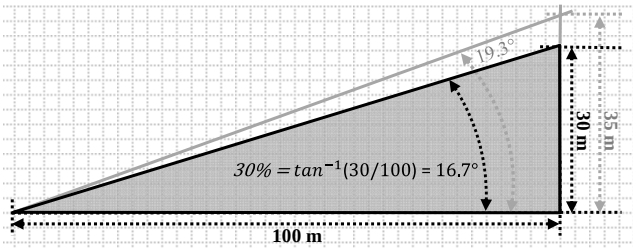

Fig. 7 Inclination for a 30% Steep Road

The tests have been conducted with 50 km/h desired velocity, 5km/h wind velocity, constant water flow in the LT-iCAC system, ~65 % pedal position, without trailer, half loaded vehicle and 1000 rpm fan-speed.

Table IV shows the ADRs for the different cooler variants at diverse ambient temperatures. Compared to the NEDC, the values for the dCAC are much lower. It is assumed that this dates back to the lower velocity of the car (but at very high torque demands) which deteriorates the heat transfer at the cooler and consequently the efficiency.

TABLE IV
ADR AT 30% INCLINATION

Ambient Temp. [°C]	ADR for dCAC [-]	ADR for iCAC [-]
5	0.696	0.954
10	0.699	0.964
20	0.706	0.962

Fig. 8 shows the ascent on the *Großglockner High Alpine Road* which is Austria's highest paved mountainous pass. The *Großglockner* has a sea height of 3798 m; hence it is the highest mountain in Austria. This track has an intense ascent, a lot of sharp turns and a vertical height of above 1000 m. For this reason, it is the perfect simulation trail for extreme conditions towards the cooling system of a car.

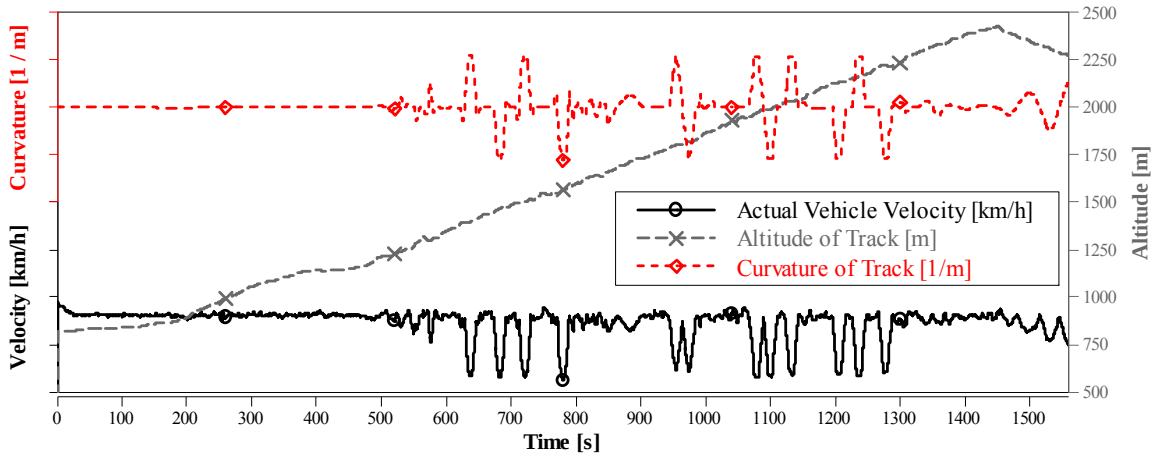

Fig. 8 Großglockner Profile for Altitude, Velocity and Curvature

The curvature was calculated on the basis of the formula for curves in the two-dimensional room, see (5).

Initially, the digital maps of the *Großglockner* course have been measured. This means that the road was described on a 2D map with its x- and y-coordinates. Then the track was separated into several parts. Polynomial coefficients were calculated for every part on the basis of the coordinates. Thus, each part was described with *f(x)* via a polynomial function up to 16 degree. *F(x)* was the basis for the derivations *f'(x)* and *f''(x),* which has been deployed in (5):

$$K(x) = \frac{f''(x)}{(1 + f'(x)2)^{3/2}} \quad (5)$$

K(x) stands for the curvature; by inverting this number, the radius for the curves can be calculated.

The *Großglockner* track has been performed with a lot of different conditions. For example, the ambient temperature was varied between -20 and +45°C. Further, the average speed was set to 50 as well as to 70 km/h. Most of the simulations even have been operated with a 1000 kg trailer.

In Table V the results for 20°C ambient temperature, 70km/h average speed and a full trailer are given. The fuel consumption dropped by 3% with the iCAC among these conditions. The NO_x-emissions were lowered even by 17% due to lower engine process temperatures.

TABLE V
GROSSGLOCKNER CYCLE RESULTS

		Direct CAC	Indirect CAC
∑ Fuel Consumption	g	2879.80	2796.30
∑ NO_x Emissions	mg	26131.40	21575.20
FC	g/km	134.90	130.90
NO_x	mg/km	1223.80	1010.20
FC	l/100km	16.20	15.80
CO_2	g/km	429.00	416.50
FC Benefit for iCAC	%		-2.97
NO_x Benefit for iCAC	%		-17.45

The fuel consumption benefits can be described by Fig. 9. Here a load step from 0 to 100 % pedal position is performed. It is important to know, that at full load, the engine with the iCAC has more air available and subsequently more fuel can be injected at equal air/fuel ratio. Hence, the desired velocity can be achieved earlier (see velocity in Fig. 9).

The better thermodynamic behaviors of the engine with an iCAC can be described as follows: Lower intake air temperatures and lower pressure drops along the CAC lead to an improved gas exchange work and to less heat losses in the cylinder. Thus, more effective energy is available at the engine's output shaft.

Beside of a better transient performance, also a fuel consumption benefit is gained due to earlier reduction of the pedal position. As seen in Fig. 9, the pedal can be released earlier, while the vehicle speed stays the same as with the dCAC. The accumulation of fuel finally leads to a benefit for the iCAC, exactly due to this phenomenon.

Further, the ambient temperature was varied as followed, with marginal lower fuel advantages for the iCAC towards high ambient temperatures:

+20°C → FC-Benefit: 3.0%
+35°C → FC-Benefit: 2.6%
+45°C → FC-Benefit: 2.0%

The same simulation on the Großglockner was conducted with an average vehicle speed of 50 km/h with as well as without a trailer. Due to a lower torque demand, the fuel consumption was solely slightly lower for both studies.

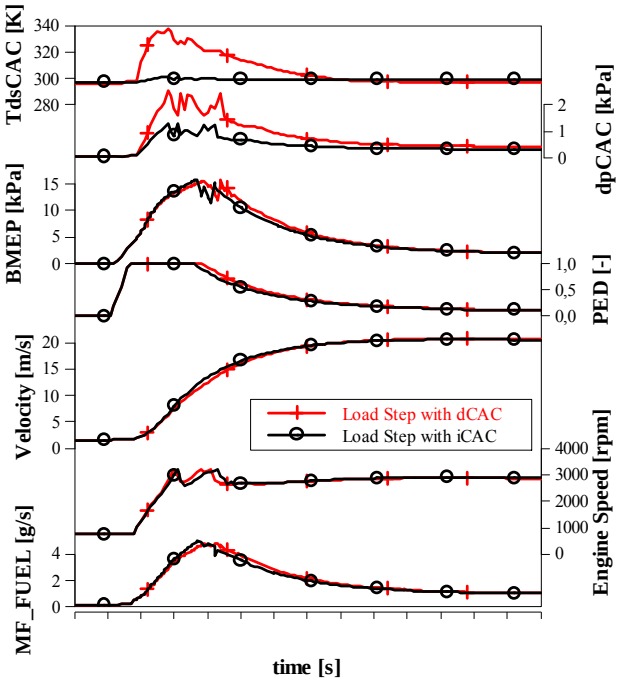

Fig. 9 FC-Benefit In Load Step

XII. CONCLUSION

In the first step *AVL BOOST®* simulations were executed for different intake plenum conditions that occur, when using a direct or an indirect charge air cooler. In doing so, special focus was put on the control of important engine parameters like constant emissions and power output at part load and constant air-fuel ratio at full load. With the gained information a quasi-stationary mean value model was built in *Matlab/Simulink®*.

With the integration of different quasi-stationary CACs and a powertrain model, different test cycles with direct as well as indirect CACs were performed. For steady state operating points and the NEDC, any significant difference was seen. The *TipIn-TipOut* test showed a fuel consumption benefit by 3.5%. Up to 3% were gained in the *Großglockner* trail.

The reason for the significant better fuel consumption is a higher volumetric efficiency and consequently a better transient performance. With the better dynamic behavior of the engine, less full load phases are required which leads in sum to a significant benefit for FC, CO_2 and NO_x. Summarized it can be told that an iCAC enables further possibilities for engine optimization as it enables the control of charge air temperature by means of a variable cooling-water mass-flow. The goal conflict for charge air cooling with respect to intake air pressure loss, thermal efficiency and available space gains a positive influence due to the iCAC.

Beside of the advantages, the following challenges in view of the total vehicle must be considered:

For a further investigation, also the electric water pump (15-100 W) of the low temperature circuit must be modeled. It is supposed to lower the FC benefit by up to 0.5%.

Also the problematic of condensation at very low intake air temperature (~25°C) must be considered with material probes. Test bed measurements showed, that the engine excellently tolerates a constant operation with up to 50% low pressure EGR which implicates a high water drop out.

Last but not least, the low temperature circuit could also be used to cool the EGR with an extension of the circuit. It is emanated, that accordingly with even lower engine process temperatures, the FC- and NO_x-benefits – as described above – can be even more boosted.

List of Abbreviations

ΔpCAC	Air Pressure Drop along the CAC
ADR	Air Density Recovery
AFR	Air/Fuel-Ratio
BCS	Boundary Condition Server
CFD	Computational Fluid Dynamics
dCAC	Direct Charge Air Cooler
Ds	Downstream
EGR	Exhaust Gas Recirculation
EP	Engine Part
FC	Fuel Consumption
HTC	Heat Transfer Coefficient
HX	Heat Exchanger
i^2CAC	Integrated Indirect CAC
iCAC	Indirect Charge Air Cooler
ICOS	Independent Co Simulation Platform
LT	Low Temperature
NEDC	New European Driving Cycle
OEM	Original Equipment Manufacturer
PWR	Power
RDE	Real Driving Emissions
ROHR	Rate of Heat Release
RTF	Real Time Factor
Us	Upstream

Acknowledgment

The authors would like to acknowledge the financial support of the "COMET K2 - Competence Centres for Excellent Technologies Programme" of the Austrian Federal Ministry for Transport, Innovation and Technology (BMVIT), the Austrian Federal Ministry of Economy, Family and Youth (BMWFJ), the Austrian Research Promotion Agency (FFG), the Province of Styria and the Styrian Business Promotion Agency (SFG).

We would furthermore like to express our thanks to our supporting industrial and scientific project partners, namely AVL List GmbH, MAHLE Behr GmbH & Co. KG, Continental Automotive GmbH and to the Graz University of Technology.

References

[1] REO Inductive Components AG, "Wasserkühlung für induktive und ohmsche Komponenten", www.reo.de, downloaded on 24/10/14.
[2] Merker, G.P., Schwarz, C., Stiesch, G., Otto, F., „Verbrennungsmotoren, Simulation der Verbrennung und Schafstoffbildung", Teubner, 3.Auflage, Wiesbaden, 2006
[3] S. Burgold, J.-P. Galland, B. Ferlay, L. Odillard, Valeo Powertrain, "Modulare Indirekte Ladeluftkühlung für Verbrennungsmotoren", MTZ 11 2012, Volume 73
[4] K.-E. Hummel, B. Huurdeman, J. Diem, Ch. Saumweber, Behr, Ansaugmodul mit Indirektem und Integriertem Ladeluftkühler, MTZ 11 2010, Volume 71
[5] E. Pantow, A. Kleber, R. Lutz, MAHLE GmbH, "Vorteile indirekter Kühlsysteme für schwere Nutzfahrzeuge", ATZ 09 2014, Volume 116
[6] AVL BOOST User Guide Version 2010.1, Edition 03/2011, Graz, 2011
[7] R. Gneiting, Th. Heckenberger, Ch. Sauer, Behr GmbH, "Virtual Thermal Management in Cars – Requirements and Implementation", 6th FKFS Conference: Progress in Vehicle Aerdoynamics and Thermal Management, Stuttgart, 2007
[8] R. Gneiting, Th. Heckenberger, Ch. Sauer, Behr GmbH, "Virtual Thermal Management in Cars – Requirements and Implementation", 6th FKFS Conference: Progress in Vehicle Aerdoynamics and Thermal Management, Stuttgart, 2007